



OPEN

Preparation of glass-ionomer cement containing ethanolic Brazilian pepper extract (*Schinus terebinthifolius* Raddi) fruits: chemical and biological assays

Isabelle C. Pinto¹, Janaína B. Seibert², Luciano S. Pinto², Vagner R. Santos³, Rafaela F. de Sousa¹, Lucas R. D. Sousa^{1,4}, Tatiane R. Amparo⁵, Viviane M. R. dos Santos¹, Andrea M. do Nascimento¹, Gustavo Henrique Bianco de Souza⁵, Walisson A. Vasconcellos⁶, Paula M. A. Vieira⁴ & Ângela L. Andrade¹✉

Plants may contain beneficial or potentially dangerous substances to humans. This study aimed to prepare and evaluate a new drug delivery system based on a glass-ionomer-Brazilian pepper extract composite, to check for its activity against pathogenic microorganisms of the oral cavity, along with its in vitro biocompatibility. The ethanolic Brazilian pepper extract (BPE), the glass-ionomer cement (GIC) and the composite GIC-BPE were characterized by scanning electron microscopy, attenuated total reflectance Fourier transform infrared spectroscopy (ATR-FTIR), and thermal analysis. The BPE compounds were identified by UPLC-QTOF-MS/MS. The release profile of flavonoids and the mechanical properties of the GIC-BPE composite were assessed. The flavonoids were released through a linear mechanism governing the diffusion for the first 48 h, as evidenced by the M_t/M_∞ relatively to \sqrt{t} , at a diffusion coefficient of $1.406 \times 10^{-6} \text{ cm}^2 \text{ s}^{-1}$. The ATR-FTIR analysis indicated that a chemical bond between the GIC and BPE components may have occurred, but the compressive strength of GIC-BPE does not differ significantly from that of this glass-ionomer. The GIC-BPE sample revealed an ample bacterial activity at non-cytotoxic concentrations for the human fibroblast MRC-5 cells. These results suggest that the prepared composite may represent an alternative agent for endodontic treatment.

It is established that the bacterial flora of the gingival crevice may help better understand the etiology of periodontal disease¹ and, thus, orient its treatment by controlling this microflora. Although systemic administration of conventional antibiotics has been proved to be a useful method of controlling such a sub-gingival infection², the challenge now turns to be preventing the indiscriminate antibiotic therapy, which may very likely lead to systemic side-effects, appearance of resistant strains, and superimposed infections. This idea strongly supports the search of clinically more efficient alternative treatments, with no significant collateral effect to the patient: it is envisaged to develop a suitably designed mini-support to carry and locally deliver the pharmacological principle at a specific point in the buccal cavity. The supporting material anchoring the active principle must be biologically safe and allows delivering the therapeutic drug at a rate assuring its optimum anti-biotic action.

The use of phytotherapeutic principles to treat, cure and prevent human diseases is one of the oldest forms of medicinal practice of the humankind. Nevertheless, since the appearance of synthetic drugs, starting by the aspirin, in 1897, there has been a decreasing interest in plant-derived therapeutics³. Herbal medicine was seen

¹Departamento de Química, Universidade Federal de Ouro Preto, UFOP, Ouro Preto 35400-000, Brazil. ²Departamento de Química, Universidade Federal de São Carlos, UFSCar, São Carlos 13565-905, Brazil. ³Departamento de Clínica, Patologia e Cirurgias Odontológicas, Universidade Federal de Minas Gerais, UFMG, Belo Horizonte 31270-901, Brazil. ⁴Departamento de Ciências Biológicas, Universidade Federal de Ouro Preto, UFOP, Ouro Preto 35400-000, Brazil. ⁵Laboratório de Fitotecnologia, Universidade Federal de Ouro Preto, UFOP, Ouro Preto 35400-000, Brazil. ⁶Departamento de Odontologia Restauradora, Universidade Federal de Minas Gerais, UFMG, Belo Horizonte 31270-901, Brazil. ✉email: angelaleao@ufop.edu.br

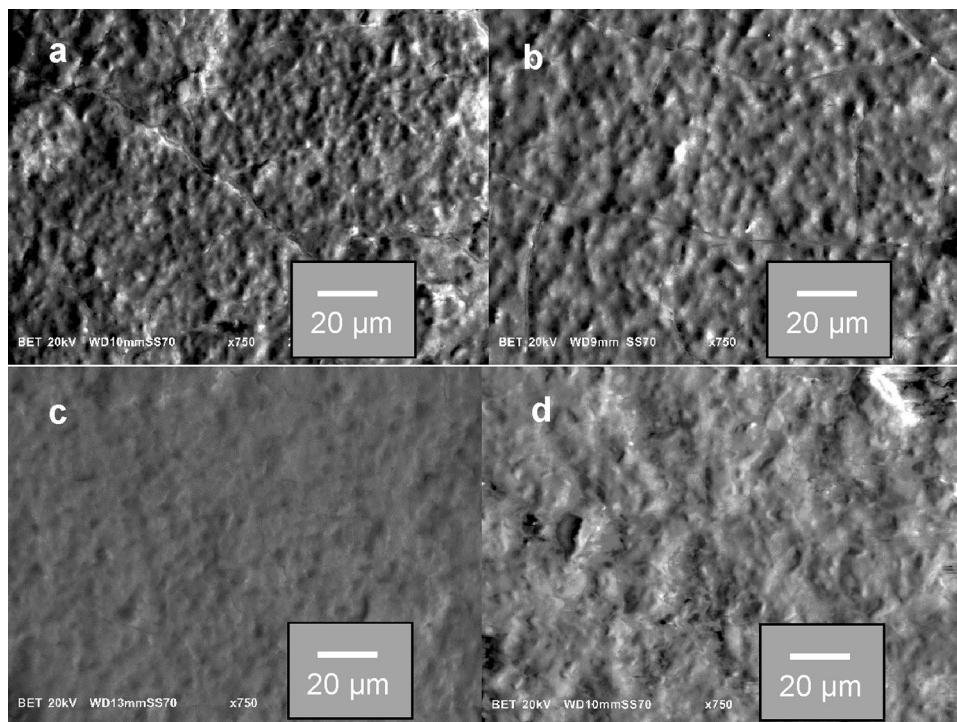


Figure 1. Microphotographs of glass-ionomer cements samples: (a) GIC and (b) GIC-BPE, before immersion in SBF solution; and (c) GIC and (d) GIC-BPE, after immersion in SBF solution for 96 h.

as an “unqualified, non-scientific and primitive medicinal practice”, used by people without access to the “real” medicine³. However, in more recent years phytotherapeutics have become again popular, which can be seen by the number of scientific papers published on this subject. Nevertheless, some plants have the potential to be poisoning to humans. Plants produce a plethora of metabolic compounds acting to self-protect them from invasion by microorganisms and viruses as well as from the herbivorous macro-fauna⁴. These complex substances include several classes of compounds, some of which are lethal to humans even if consumed in minute quantities⁴. Because of this potential toxicity, it is always important to perform biocompatibility testing when trying the use of a given plant extract against microorganisms.

Schinus terebinthifolius Raddi, from the Anacardiaceae family, is a medicinal plant, native of the Brazilian flora, and is commonly known as Brazilian pepper or Aroeira. Previous studies have shown that *S. terebinthifolius* does contain phenolic compounds with different biological activities, including antimicrobial, antiulcerogenic, anticancer, antihistamine, antihypertensive, antihyperalgesic, wound healing, anti-inflammatory and antioxidant activities in different models^{5–13}.

Despite of the various studies of Brazilian pepper extract (BPE) in dentistry, there are very few studies dealing with the ethanolic extract of Brazilian pepper fruit incorporated into GICs and no study at all on the releasing profile of the flavonoids of the pepper extract, incorporated into the ionomer, has been reported. Taking into regard that the drug release profile is critical to allow proposing changes in the synthesis protocol towards its better clinical use¹⁴, the purpose of this work was to add the BPE to the GIC, in an effort to know more in deep about the enhanced antibacterial activity mainly due to the flavonoids and to attempt developing a new therapeutic alternative agent, which may be used in endodontic treatments.

Being the focus of this work the development of a phytotherapeutic anti-biotic carrier, the glass-ionomer cement (GIC), a material basically consisting of a basic glass and acidic polymer, as previously proposed by Wilson and Kent¹⁵, was now studied in more details. The glass-ionomer was chosen for its ability, from among many of its potential uses, to act as drug delivery supporting systems¹⁶.

Results

Characterization of the samples. Figure 1 shows the SEM image of GIC and GIC-BPE samples, before (Fig. 1a,b, respectively) and after (Fig. 1c,d, respectively) immersion in SBF. There were significant differences in the initial surface roughness of the samples before and after immersion in SBF. After drug loading, the samples were apparently smoother.

Figure 2 shows the ATR-FTIR absorption spectra of GIC, BPE and GIC-BPE samples. The characteristic peaks are listed in the Table 1.

The weight loss (TG) and derivative weight loss (DTG) curves of the GIC, BPE and GIC-BPE samples under an air environment are illustrated in Fig. 3. The TG for the GIC sample (Fig. 3a) shows two main stages of weight loss at the temperature intervals of 30–150 °C and 330–580 °C. The total loss up to 600 °C amounted to about 25.6% of the initial mass.

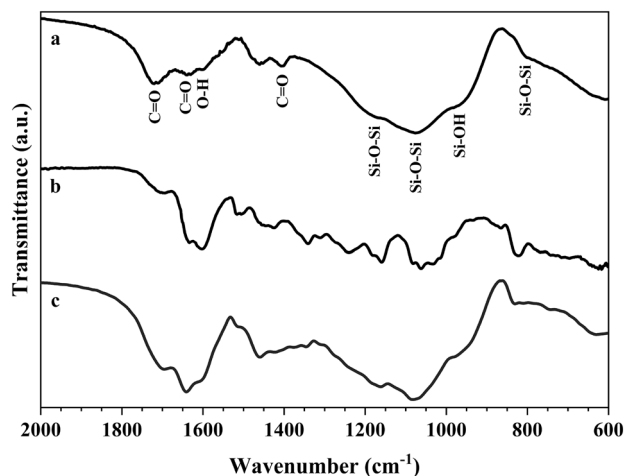


Figure 2. ATR-FTIR spectra of: (a) GIC, (b) BPE, and (c) GIC-BPE.

Sample	Bands (cm ⁻¹)	Preliminary assignments	Main attribution	References
GIC sample (Fig. 2a)	1700 and 1650	C=O stretching	Carbonyl group	17
	1604	OH deformation	Aromatic ring vibration	17
	1402	C=O stretching	Carboxylate for surface hydroxyl group	18
	1170, 1080 and 800	Si-O-Si asymmetric stretching and Si-O-Si bending	Siloxane	18–20
	950	Si-OH stretching	Silanol	18–20
BPE sample ^a (Fig. 2b)	1680	C=O stretching	Phenolic compounds and flavonoids	21
	1150–1050 cm ⁻¹ and 900–1300 cm ⁻¹	C-OH and CH groups, respectively	Phenolic compounds and flavonoids	21

Table 1. The preliminary assignments of ATR-FTIR absorption spectra of GIC, BPE and GIC-BPE samples.

^aThe broad absorption bands obtained from *Schinus terebinthifolius* Raddi represent the substantial overlap of absorption bands of various components with different contents.

The pyrolysis process of *S. terebinthifolius* dry extract (BPE sample) showed four distinct mass loss zones (Fig. 3b).

The GIC-BPE specimen (Fig. 3c) presented weight losses at the temperature intervals of 30–270 °C, 270–391 °C and 391–600 °C (26.61%, 29.35% and 28.00%, respectively).

The DTA curve for the GIC sample (Fig. 3a) shows the presence of an exothermic peak at 472 °C. The DTA curve for the BPE sample (Fig. 3b) initially indicate an endothermic peak. After this, it shows an exothermic event. The DTA curve for the GIC-BPE sample (Fig. 3c) shows the presence of an exothermic peak at 470 °C.

To our knowledge, there is no study investigating the mechanical properties of the GIC-BPE composite. Our study shows that the incorporation of about 38 wt% BPE decreased the compressive strength of the GIC based composite from 176.60 ± 6.46 MPa to 161.17 ± 5.01 MPa in the composite GIC-BPE.

Phytochemical analyses revealed that alkaloid, anthraquinone, carbohydrate, and saponin were absent. The test was based on the colour changes after the reaction of the extract with standard reagents. The BPE sample presented a positive result for flavonoids, tannin and terpenoids.

Results of analyses performed on ethanolic BPE show that the total phenolic content was 60.09 ± 7.65 mg of galic acid/g of sample and the total flavonoids content was 1.88 ± 1.01 mg of quercetin/g of sample. Uliana et al.¹³ found a similar result for essential oil extracted from Brazilian pepper.

The chemical profile of BPE was performed using UPLC-QTOF-MS/MS analysis and the molecular formula of precursor ions (MS1 spectra) were calculated (accurate 3 ppm). Then, ions-fragment analysis (MS2 spectra) and proposed fragmentation mechanism were performed using molecular annotation from different metabolite databases (FooDB, PlantCyc, ChEBI, LipidMAPS, DrugBank, KNApSACk, NANPDB, PubChem, UNPD, and METLIN) and confidence literature. Chromatogram of the BPE (Fig. S1) and the MS1 and MS2 data for each compound are described in the supplementary material (Figs. S2–S59). According to Table 2, 27 compounds were suggested, and their chemical structures are represented in the Fig. 4.

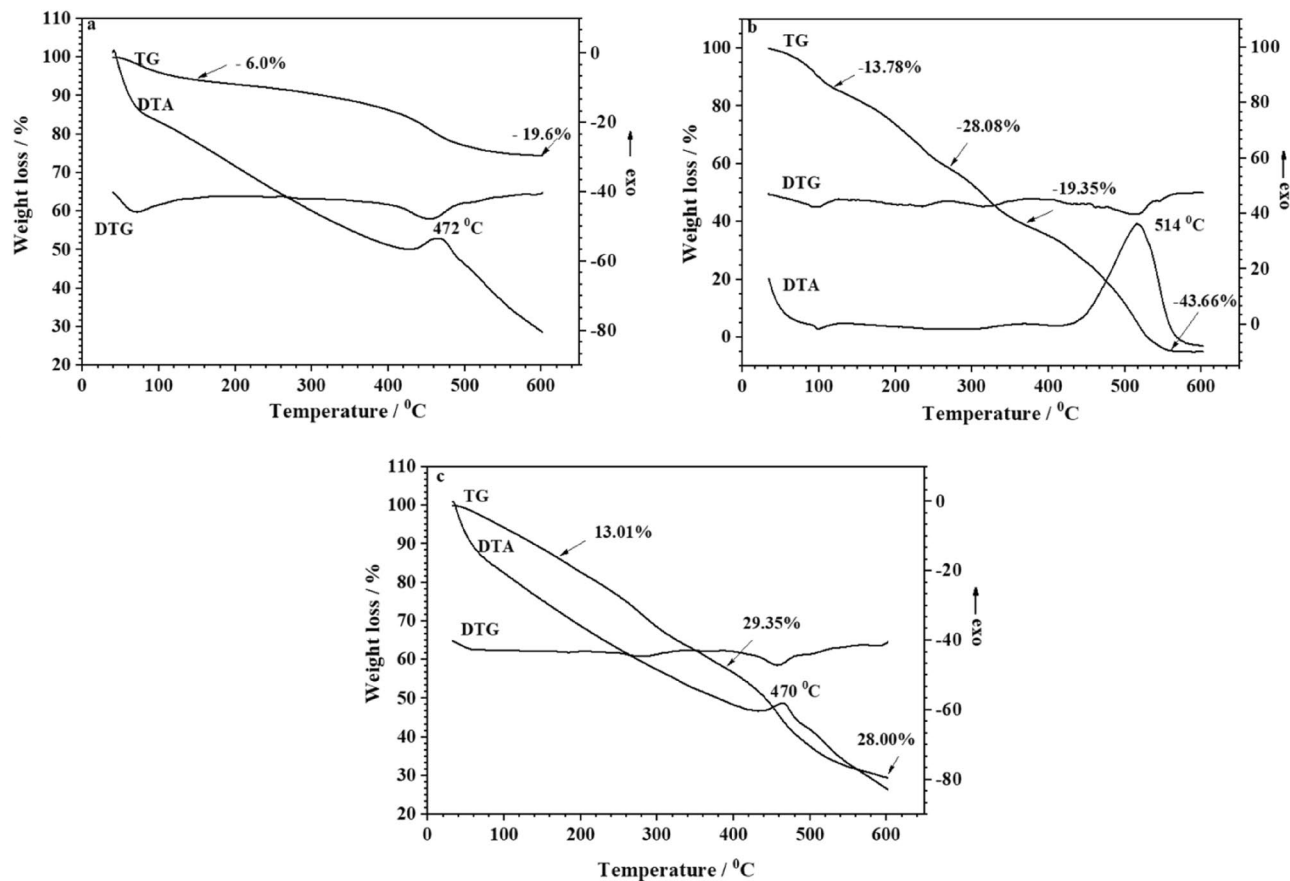


Figure 3. TG/DTG/DTA diagrams of samples: (a) GIC, (b) BPE, (c) GIC-BPE, before immersion in SBF.

Drug release from GIC-BPE composite. Figure 5a shows the curve of flavonoid release in two stages. The first stage corresponds to a rapid first release of the drug; in the second stage, a more controlled and slower behavior is observed until approximately 96 h.

The drug releasing profile was used to determine M_t/M_∞ values. The 96 h-release value was taken as a reasonable estimation of the M_∞ value. This plot was used to determine the diffusion coefficient through the known Stefan approximation, meaning inserting into the equation: $D = s^2\pi l^2/4$, where s is the slope of the diffusion plot and l is the specimen thickness. The release data is shown in Fig. 5b.

Cytotoxicity testing showed that the GIC-BPE and GIC samples exhibit lower cytotoxicity than the BPE sample. Furthermore, all samples showed low cytotoxicity for MRC-5 cells.

The GIC-BPE at concentrations 16, 31, 62, 125 and 250 $\mu\text{g}/\text{mL}$ showed no cytotoxic effect for MRC-5 cells, with cell viability above 70%⁴⁵.

The extracted essential oil from the *S. terebinthifolius* is reportedly used to treat respiratory illnesses, mycosis and candida infections⁴⁶; its activity is assigned to the high concentrations of monoterpenes, phenols and flavonoids¹¹. Despite of this, to the best of our knowledge, there is no study about the use of the ethanolic extract from *S. terebinthifolius* fruit against pathogenic microorganisms of the oral cavity. In this work, we evaluated the activity of ethanolic extract from fruits *S. terebinthifolius* extract in a releasing device to form a therapeutic system to act against common pathogens in the human oral cavity. The advantage of this device is that it provides slower and longer release of the drug.

The agar diffusion test (Fig. 6) showed that the BPE had significant antimicrobial activity against all bacterial species evaluated. The GIC-BPE sample had lower antimicrobial activity than the BPE sample and has no antimicrobial activity against *Candida albicans*. No inhibition zone was observed when ethanol was tested alone.

Discussion

The ATR-FTIR spectrum for the GIC-BPE sample (Fig. 2c) shows bands of GIC and of BPE, which indicates that the Brazilian pepper extract was incorporated into the ionomer. In addition, there was overlapping of some bands. Despite this, multiple bands of the BPE sample and some bands of the GIC sample disappeared in the GIC-BPE sample indicating that a probable intermolecular interaction exists between the glass-ionomer and functional groups of flavonoid compounds from BPE.

The first weight loss for the GIC sample was attributed to the removal of water from the surface. This stage was reflected in the DTG curve in this region (Fig. 3a). The mass loss at the higher temperature represents not only the degradation of any evolving polyalkenoate polymer but also the decomposition of unreacted components^{47–49}.

No.	RT (min)	[M-H] ⁻ (m/z)	Formula	Error (ppm)	Ions-fragment (m/z)	Annotation	Class	References
1	0.91	343.0667	C ₁₄ H ₁₆ O ₁₀	0.6	191.06; 169.01; 125.02; 93.04	Theogallin	GD	22
2	0.92	331.0668	C ₁₃ H ₁₆ O ₁₀	0.9	271.05; 241.04; 211.03; 169.01; 125.02	Glucogallin	GD	23
3	3.05	325.0558	C ₁₄ H ₁₄ O ₉	-0.6	185.02; 173.05; 169.01; 124.02; 111.05	5-Galloylshikimic acid	GD	24
4	3.26	495.0775	C ₂₁ H ₂₀ O ₁₄	0.0	343.07; 325.06; 191.06; 173.05; 169.01; 125.02	3,4-Di-O-galloylquinic acid	GD	25
5	3.42	483.0773	C ₂₀ H ₂₀ O ₁₄	-0.4	331.07; 271.05; 211.02; 169.01; 125.02	1,2-Digalloyl-β-D-glucopyranose	GD	26
6	4.30	321.0247	C ₁₄ H ₁₀ O ₉	0.0	169.01; 125.03	Digallic acid	GD	27
7	4.76	477.0669	C ₂₁ H ₁₈ O ₁₃	0.0	325.05; 307.04; 201.06; 169.01; 125.02	3,5-Di-O-galloylshikimic acid	GD	24
8	4.76	635.0882	C ₂₇ H ₂₄ O ₁₈	-0.3	521.02; 483.08; 465.07; 331.07; 271.05; 169.01	1,2,6-Trigalloyl-β-D-glucopyranose	GD	28
9	5.39	473.0353	C ₂₁ H ₁₄ O ₁₃	-0.6	321.03; 169.01; 125.02	Trigallic acid	GD	29
10	5.39	615.0986	C ₂₈ H ₂₄ O ₁₆	0.0	463.09; 301.03; 271.03	2''-O-Galloylhyperin	GD/ FL	30
11	5.44	787.0987	C ₃₄ H ₂₈ O ₂₂	-0.9	635.09; 617.08; 483.08; 465.07; 447.06; 403.05; 179.03	1,2,3,6-Tetragalloyl-β-D-glucopyranose	GD	31
12	5.47	169.0139	C ₇ H ₆ O ₅	1.2	125.02; 107.01; 97.03; 79.02	Gallic acid	GD	32
13	5.49	629.0778	C ₂₈ H ₂₂ O ₁₇	-0.2	583.05; 477.07; 325.06; 169.01	Trigalloylshikimic acid	GD	24
14	5.65	463.0873	C ₂₁ H ₂₀ O ₁₂	-0.9	317.03; 316.02; 271.02; 164.08	Myricitrin	FL	33
15	5.75	441.0821	C ₂₂ H ₁₈ O ₁₀	-0.2	315.03; 289.07; 245.08; 137.03	Catechin 3-O-gallate	GD/CA	34
16	6.01	433.0774	C ₂₀ H ₁₈ O ₁₁	0.7	313.09; 301.04; 300.03	Avicularin	FL	35
17	6.17	447.0927	C ₂₁ H ₂₀ O ₁₁	0.0	300.03; 271.02; 255.03; 243.03; 151.00; 135.01	Quercitrin	FL	36
18	6.41	417.0819	C ₂₀ H ₁₈ O ₁₀	-0.7	284.03; 255.03; 227.03	Kaempferol 3-O-α-L-arabinopyranoside	FL	37
19	6.80	287.0559	C ₁₅ H ₁₂ O ₆	1.0	259.06; 177.06; 151.00; 125.02; 83.01	Eriodictyol	FL	38
20	6.88	585.0881	C ₂₇ H ₂₂ O ₁₅	0.2	301.04; 283.05; 169.01; 151.00; 125.02	Quercetin 3-(2''-galloyl-α-L-arabinopyranoside)	FL	39
21	6.96	197.0450	C ₉ H ₁₀ O ₅	0.0	169.02; 124.02; 106.01; 78.01	Ethyl gallate	GD	40
22	7.03	349.0560	C ₁₆ H ₁₄ O ₉	0.0	197.05; 169.01; 125.02; 124.02	2,3,5,7-Tetrahydroxychroman-3-O-gallate	GD	-
23	7.72	703.1668	C ₃₆ H ₃₂ O ₁₅	0.7	541.11; 497.12; 389.10; 311.06 229.05	Fukugentin-7''-glucose	GD/FL	-
24	7.77	301.0348	C ₁₅ H ₁₀ O ₇	0.0	193.01; 178.99 151.00	Quercetin	FL	41
25	9.23	537.0821	C ₃₀ H ₁₈ O ₁₀	-0.2	417.06; 375.05; 331.06; 159.05	Amentoflavone	FL	42
26	9.55	539.0980	C ₃₀ H ₂₀ O ₁₀	0.4	413.07; 387.09; 319.02; 293.05; 267.07; 251.04; 225.06; 161.02; 125.02	Volkensiflavone	FL	43
27	9.63	541.1133	C ₃₀ H ₂₂ O ₁₀	-0.4	415.08; 389.10; 351.09; 311.06; 243.07; 201.06; 159.05; 125.02	Isochamaejasmin	FL	44

Table 2. Detected compounds from ethanolic extract of *Schinus terebinthifolius* (Brazilian pepper) by UPLC-QTOF-MS/MS. CA catechin, FL flavonoid, GD gallic acid derivative.

For the BPE sample (Fig. 3b), the mass loss event in the first zone (30–118.40 °C) is assignable to the loss of water and light volatile compounds in the sample (13.78%) and a peak on the DTG curve was observed around 94.1 °C. The other zone (118.40–272.17 °C) is associated with the thermal decomposition of carbohydrates and other organic compounds present in the plant⁵⁰. In the third zone, the organic materials were gradually released (19.35%), resulting in a large mass loss and the formation of the main pyrolytic products. As shown in the derivative weight loss (DTG), several stages of decomposition could be distinguished. Studies of phytochemicals identified the presence of tannins, flavonoids, and terpenoids in the species under study. In the last stage, between 370.42 and 600 °C, these carbonaceous matters decomposed⁵¹. More than 43% of the weight loss of the sample occurred in this stage.

While the GIC sample lost about 26% by mass up to 600 °C, the GIC-BPE sample lost about 84%. Most of this difference in mass loss is due to the pepper extract incorporated in the GIC. Interestingly, although the GIC-BPE sample has a large amount of BPE, the peak shown on the DTG curve of the GIC-BPE sample is at a temperature similar to that of the GIC sample.

More insights about the thermal decomposition peaks can be obtained from DTA curves (Fig. 3). The endothermic peak of the DTA profile for the BPE sample (Fig. 3b) is due to a dehydration event corresponding to the first mass loss of the TG curves. The exothermic event is likely due to the degradation and oxidation of organic matter and corresponds with the fourth mass loss observed in the TG curve. These results have been observed by other authors with starches from several botanical origins and treatments^{52,53}. The DTA curve for the GIC-BPE sample (Fig. 3c) shows the presence of an exothermic peak at 470 °C. It may be that the exothermic peak of the BPE sample (514 °C) has shifted to a lower temperature (470 °C). This decrease in the thermal stability of BPE suggests a chemical interaction between the components of the extract (BPE) with the glass-ionomer, confirming the ATR-FTIR result.

The compressive strength of the GIC-BPE sample was lower than that of the GIC sample. Similar results were reportedly found for other additives, including propolis, antimicrobials and bioactive glasses^{16,54,55}. Whatever its chemical origin is, this trend to lower its therapeutic strength is widespread and is characteristically associated

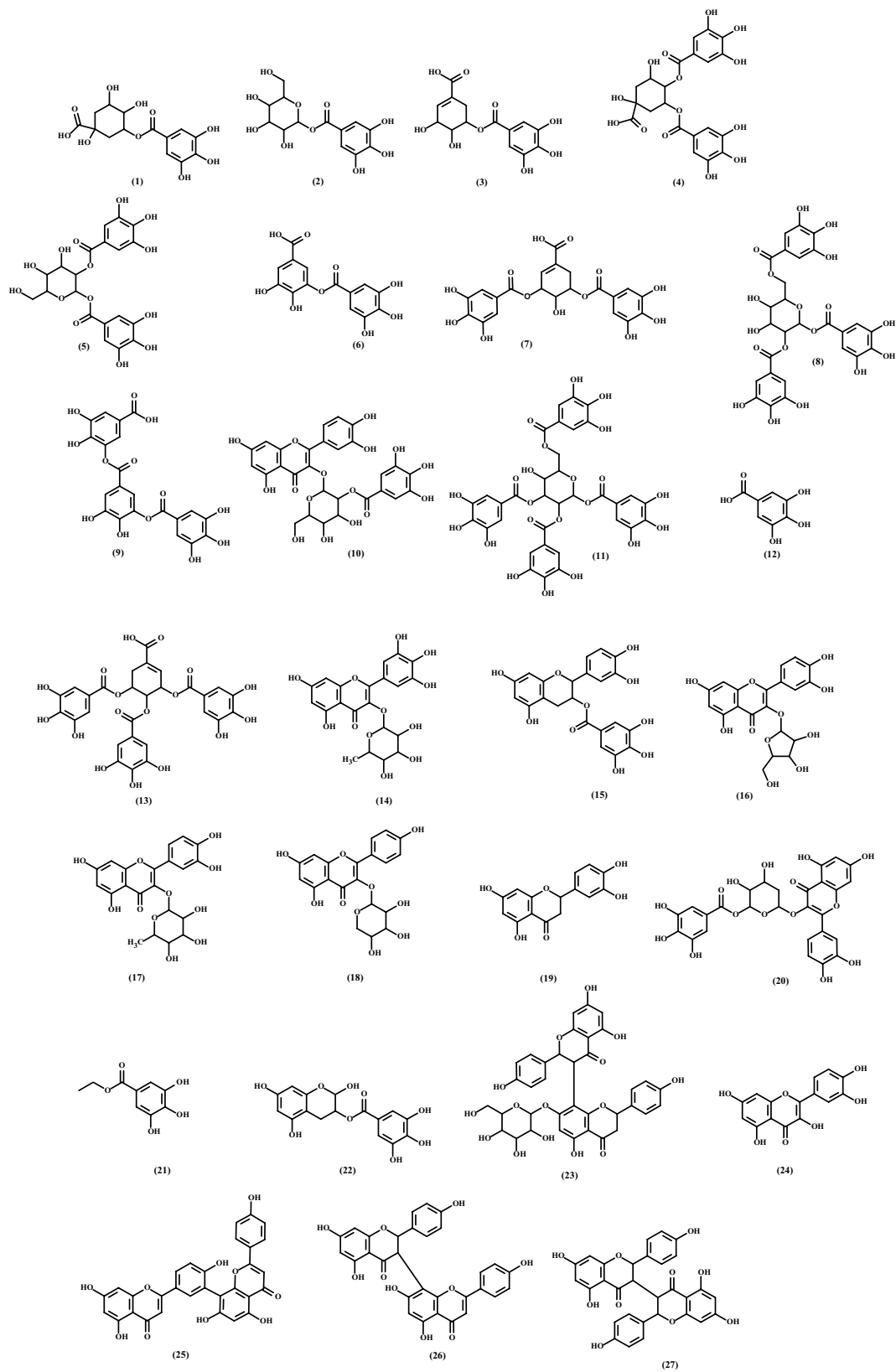


Figure 4. Chemical structures of the proposed compounds 1–27 present in the ethanolic extract of *Schinus terebinthifolius* (Brazilian pepper).

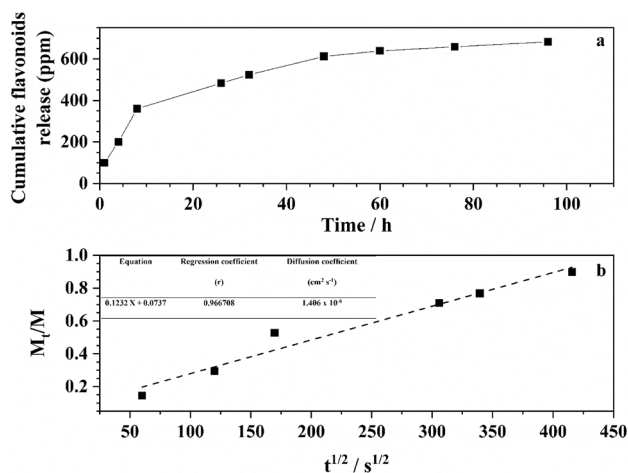


Figure 5. (a) Proportion of released flavonoid for sample GIC-BPE, (b) diffusion equation, regression coefficients, diffusion coefficient for the flavonoids release from GIC-BPE, and diffusion plot for flavonoids extracted from the GIC-BPE sample.

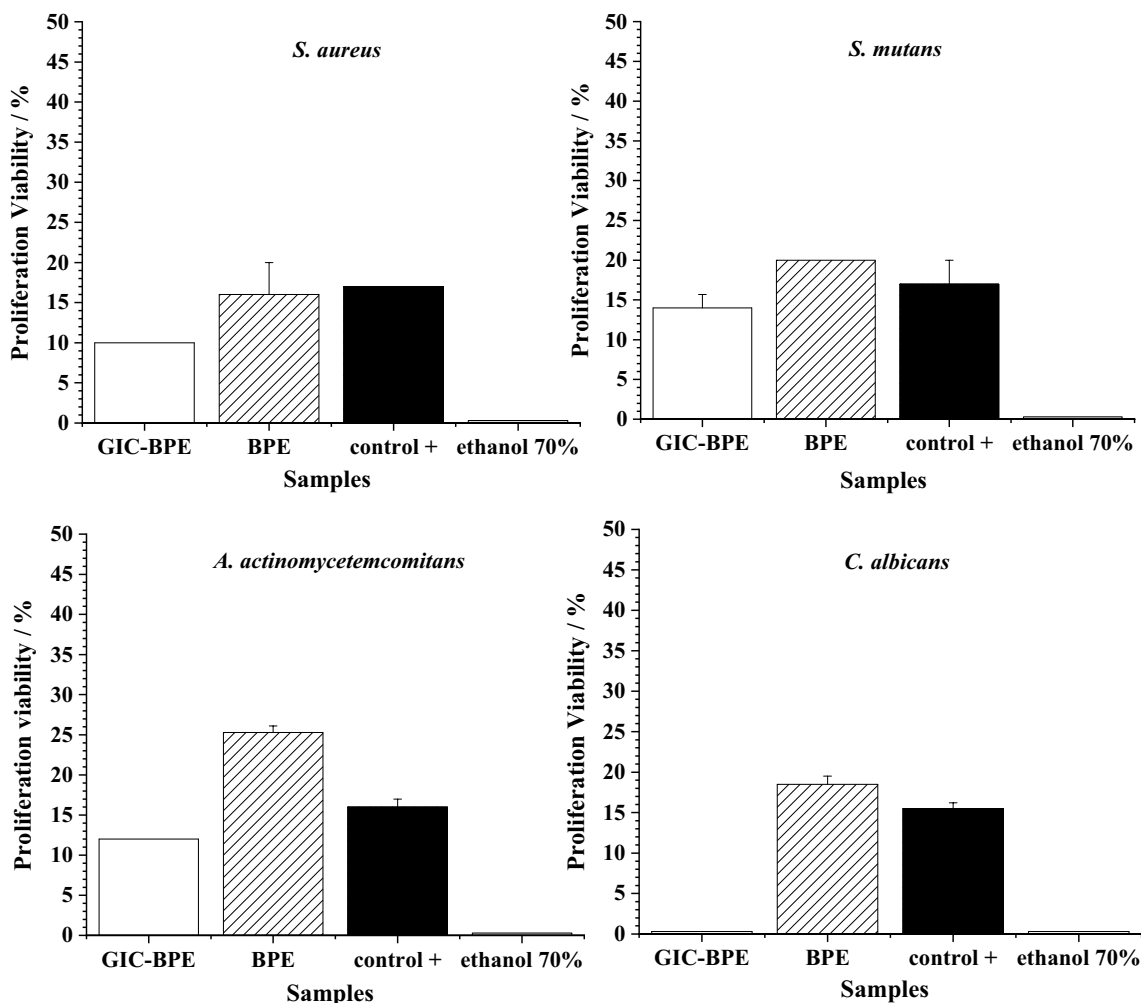


Figure 6. Susceptibility of samples of: a glass-ionomer—Brazilian pepper extract cylindrical pellet (GIC-PE), and blank disks soaked in ethanolic Brazilian pepper extract (BPE), positive control (chlorhexidine or nystatin for bacteria or yeast, respectively), and solvent control (ethanol 70%), against *S. aureus*, *S. mutans*, *A. actinomycetemcomitans*, and *C. albicans*. Media and standard deviation (MD ± SD), mean of three experiments.

to the inhibition of the setting reaction due to the presence of the additive. It seems that the reducing mechanical properties of the cements, on adding additives, is due to their concentrations and to even small amounts of the additive. This decrease appears to be related to chemical interactions between the drug and the glass ionomer chemical components. Thus, the cationic compounds based on quaternary ammonium salts, such as benzalkonium chloride and cetyl pyridinium chloride, have a particular ability to do this via interaction with the poly(acrylic acid) component^{56,57}. However, this effect has also been observed for neutral species, such as methanol⁵⁸, 2-hydroxyethyl methacrylate⁵⁸ and sodium chloride⁵⁹. The chemical compounds of the ethanolic extract of *S. terebinthifolius* are likely to interact with the glass ionomer. This was evidenced from the FTIR and thermogravimetric results.

Several factors can determine the chemical composition of a plant, such as availability of nutrients, and organic matter in the soil⁶⁰. Because of this, a chemical analysis was performed by UPLC–QTOF–MS/MS (Fig. 4 and Table 2) to identify the components of the ethanolic extract so obtained. The characterized compounds were classified into three groups: gallic acid derivative, flavonoid and catechin. These data are in agreement with the previous phytochemical analysis, since galloyl derivatives can also be classified as tannins.

The galloyl derivatives fragmentation pattern is mainly characterized by ions at m/z 191.06, 169.01 and 125.02 (Fig. S60). The loss of gallic acid and quinic acid structures is related to the first and second fragment ions, respectively. Finally, the loss of CO_2 corresponds to the last ion⁶¹. On the other hand, flavonoids do not show a fragmentation pattern since it can vary according to their classification. In the Fig. S61 is represented an example of fragmentation from flavonoid that was not found in the literature but that was proposed as fukugentin-7"-glucose. In addition, a proposed fragmentation of catechin 3-O-gallate is described in the Fig. S62.

Among the suggested compounds, gallic acid, quercetin and quercitrin have already been reported for *Schinus molle* that showed a broad spectrum of antimicrobial activity⁶². In this same way, ethanolic extract from fruits and leaves of *S. terebinthifolius* showed high potential against *E. coli* and this data can be related to the presence of ethyl gallate, which was one of the main compounds reported⁶³. Other proposed substances, such as myricitrin⁶⁴, catechin 3-O-gallate⁶⁵, avicularin⁶⁶, and amentoflavone⁶⁷ also demonstrated action against microorganisms. Thus, all of these data support the findings of our work.

The curve shows a rapid first release of flavonoids (Fig. 5). It is suggested that this rapid initial release occurs as some drugs became trapped on the surface of the support, during its preparation⁶⁸, to be freed immediately upon activation in a proper medium. In a second stage, a more controlled and slower behavior is observed. This slower release suggests an interaction between the GIC and the flavonoids, as it is evidenced by the FTIR, thermogravimetric and mechanical data.

The resulting diffusion plot relating M_t/M_∞ and \sqrt{t} was found to be linear for about the first 48 h, indicating that the release occurred through a diffusion-governed mechanism following the Fick's law of diffusion (Fig. 5b). Several studies have reported the antimicrobial compounds being incorporated into glass-ionomer cements. Diffusion coefficients values from some of these studies were: 6.16×10^{-9} and 1.39×10^{-9} , for 3% the cetylpyridinium chloride and 3% benzalkonium⁶⁹; 4.4×10^{-8} for the 1% sodium fusidate⁷⁰ and 3×10^{-7} for the 10% chlorhexidine $\text{cm}^2 \text{s}^{-1}$ ⁷¹ release from glass ionomer. Several reportedly results^{70,71} have shown that increasing the concentration of a given drug tends to decrease the diffusion coefficient. As a comparatively remarkable result, in this work, the concentration of flavonoids in the GIC-BPE sample is approximately 0.5% and the diffusion coefficient was found to be $1.406 \times 10^{-6} \text{ cm}^2 \text{ s}^{-1}$.

The results of cytotoxicity these tests showed that the viability of the MRC-5 cells was BPE concentration dependent, and the cytotoxic concentration for 50% of the cells (CC_{50}) was 2696, 701.3 and 154.8 $\mu\text{g/mL}$ for GIC, GIC-BPE and BPE, respectively.

The lower antimicrobial activity of GIC-BPE sample, compared to BPE sample, can be explained by the fact that in the GIC-BPE, the BPE is incorporated into the ionomer, which makes the delivery slower.

According to Jakobek⁷², the detected flavonoids and phenolic compounds in plant extracts act as antimicrobial agents against various human pathogens. The mechanism of action of polyphenols on microorganisms is still poorly understood, and some authors suggest that polyphenol acts by reducing the iron availability, inhibiting protein expression, changing the cell membrane permeability and fluidity^{73–75}.

The GIC-BPE sample showed antimicrobial activity at non-cytotoxic concentrations to human fibroblasts cells. Therefore, the obtained results suggest that this extract can be an efficient alternative for the treatment of infections of the oral cavity, such as stomatitis, dental cavities and periodontitis caused by *S. aureus*, *S. mutans*, *A. actinomycetemcomitans*, and *C. albicans*.

Material and methods

Material. All GIC samples were prepared from Maxxion C. All other reagents (analytical grade) were used as received.

Preparation of ethanolic extracts from the *Schinus terebinthifolius* Raddi fruits (BPE) and from the GIC-BPE sample. Fruits of *S. terebinthifolius* Raddi were collected in Ouro Preto, Minas Gerais State, Brazil ($20^\circ 23' 8'' \text{ S}$ and $43^\circ 30' 13'' \text{ W}$) in April 2019. A voucher specimen was identified and deposited at the UFOP José Badini herbarium under the code OUPR31536.

Extraction involved macerating the fruits (1.08 kg) at room temperature with ethanol 95% (2 L, 2 consecutive extractions over 24 h). The extracted solutions were filtered and submitted to vacuum evaporation to afford 123.64 g of ethanolic crude extract.

The GIC was prepared according to the manufacturer's instructions by mixing the powder and liquid in a 1:1 ratio. The drug-free samples were labelled GIC.

The BPE was incorporated into the glass-ionomer powder and mixed for 15 s with a spatula. Then, the liquid phase of the glass-ionomer was added to the mixture and homogenized to slurry. The resulting paste was then dried in an oven at 37 °C for 1 h. The amount of BPE initially added was approximately 38 wt%. This sample was labelled GIC-BPE.

Characterization techniques of the samples. The morphology of the GIC and GIC-BPE samples was studied by SEM (Jeol JSM 6010LA). Prior to analysis, the samples were fastened to a sample holder with the help of a double carbon ribbon and covered with carbon. The sample structure information was collected by attenuated total reflectance Fourier transform infrared spectroscopy (ABB Bomen MB 3000 ATR-FTIR spectrometer, Quebec, Canada) at a resolution of 4 cm⁻¹ from 500 to 4000 cm⁻¹ and 32 scans per sample. The thermogravimetric, differential thermogravimetric and differential thermal analysis studies were carried out in a Shimadzu TG-60 thermal analyser from 25 to 700 °C at 10 °C/min in air. Al₂O₃ was used as standard. The compressive strength test of the GIC and GIC-BPE samples was performed according to ISO standardization⁷⁶ (EZ Test, Shimadzu). The compressive strength of the samples was calculated using the equation $P/\pi r^2$, where: P = load at fracture, r = the radius of the sample cylinder and π (constant) = 3.14; the values obtained were expressed in MPa. Correlations between values were analysed using a student t test, with a significance level of 5%.

Chemical tests were carried out on the BPE to identify the phytoconstituents, i.e., alkaloids, anthraquinones, flavonoids, carbohydrates, saponins, tannins and terpenoids, as per the standard procedure⁷⁷. In the chromatographic analyses the BPE was subject to clean-up process and two fractions at 50 and 100% acetonitrile (ACN) (F50ACN and F100ACN) were obtained at 200 ppm concentration (v/v) using reverse phase (1.0 g C-18 cartridge) and mobile phase ACN:H₂O (1:1). The chromatographic separation was carried out on an Agilent Zorbax SB-C18 column (3.0 × 50 acid and water—0.1% formic acid such mobile phase at flow rate of 0.3 mL min⁻¹ after injection of 3 µL of analytical solutions). The chromatographic analyzes were performed at gradient mode (5–100% of ACN during 17 min and kept under 100% ACN during 2 min). The MS1 and MS2 data were acquired in positive and negative mode and in Auto-MS/MS mode for the fragment ions by Agilent 6545 Q-TOF (Agilent Technologies Inc., Santa Clara, CA) equipped with electrospray ionization (ESI) source. The operational source parameters for TOF-MS mode were: capillary voltage of 3000 V, skimmer voltage of 65 V, fragmentation voltage of 110 V, nebulizer gas pressure of 35 psi, dry gas flow of 12 L min⁻¹, gas temperature of 320 °C, sheath gas flow of 10 L min⁻¹, sheath gas temperature of 300 °C, acquisition rate of 3 spectrum per second, and resolution of 32,000. The auto MS/MS mode was performed with table of collision energy voltage of 12 spectra per cycle, using 150–500 Da (10–15 eV), 500–1000 Da (15–30 eV), and 1000–1500 Da (30–50 eV) at medium energy of collision, whereas to high energy of collision was 150–500 Da (25–40 eV), 500–1000 Da (40–55 eV), and 1000–1500 Da (55–70 eV). MassHunter workstation software was used for acquisition and processing of the data and the ionized molecule [M–H]⁻ obtained in the TOF-MS mode were calculated.

The measurement of total phenolic content was made by the Folin-Ciocalteu method according to Bonoli et al. 2004⁷⁸ and, after incubation for 2 h, the absorbance was read at 650 nm in a microplate reader (Molecular Devices). The total phenolic content was quantified using a standard calibration curve of gallic acid (2.8–180.0 µg/mL; $r^2 = 0.9622$; $y = 0.0075x + 0.1854$). The experiment was performed in triplicate and the results were expressed as mg of gallic acid equivalents per 1 g of sample (mg GAE/g).

The measurement of total flavonoids was made by the aluminium chloride (AlCl₃) colorimetric method according to Chang et al.⁷⁹. The absorbance was read after incubation for 40 min in a microplate reader (Molecular Devices) at 405 nm. The total flavonoids were quantified using a standard calibration curve of quercetin (1.0–32.0 µg/mL; $r^2 = 0.9749$; $y = 0.0012x + 0.0371$). The experiment was performed in triplicate and the results were expressed as mg of quercetin equivalents per 1 g of sample (mg QE/g).

Drug release. To perform the flavonoid delivery test, it was necessary to prepare GIC-BPE cylindrical pellets. The pellets were prepared by compressing approximately 0.25 g of the powder, at a 0.5 ton loading for 1 min^{14,80,81}.

As already established for the release profile test^{14,80,81}, the pellets were placed in glass vials, immersed in 3 mL of a body fluid simulating solution (SBF)⁸² and incubated at 37 °C. After the intervals of 1, 4, 8, 26, 32, 48, 60, 76 and 96 h, all the solution was removed for analysis, and the pellets were immersed in 1 mL of ethanol for 10 s. Following ethanol removal, a new SBF solution was placed in the vials containing the pellets.

The amount of flavonoids extracted from BPE sample was measured using a method derived from that of Dowd^{80,83}. Preparation of the solutions for spectrophotometer analysis consisted of transferring the following to a Falcon tube: 1 mL of the SBF solution removed from the vial containing the pellet, 0.5 mL of the ethanol used to wash the pellet and 1 mL of AlCl₃ 2% in ethanol. After 10 min the Falcon tubes containing the test solutions were centrifuged at 2500 rpm for 5 min. The test solution turned yellow, and the absorbance was read at 420 nm.

The flavonoid concentration was determined by ultraviolet–visible absorption spectroscopy (UV–Vis) at 420 nm (Thermo Scientific-Genesys 840 spectrophotometer). The calibration curve of the flavonoid concentration was established by using ethanol solutions with known concentrations of quercetin.

Determination of cytotoxicity—sulforhodamine B (SRB) colorimetric assay. Human fibroblast MRC-5 cells, cultivated in RPMI 1640 medium (Sigma), were distributed in a 96-well microtiter plate using a density of 5 × 10⁴ cell/well and incubated at 37 °C with 5% CO₂ for 24 h. Cells were treated with the sample dissolved in RPMI 2% DMSO for 24 h, at concentrations ranging from 16 to 1000.00 µg/mL. Cell viability was evaluated by sulforhodamine B assay (SRB)⁸⁴. After 24 h incubation the media was removed and cells were fixed with cold 20% trichloroacetic acid for 1 h at 4 °C. The microtiter plate was washed with distilled water and dried. Thereafter, fixed cells were stained for 30 min with 0.1% SRB dissolved in 1% acetic acid. The plate was

washed again with 1% acetic acid and allowed to dry before 200 μL of 10 mM TRIS buffer (pH 10.5) was added to remove unbound dye. This was done at room temperature for ~ 30 min. Sample absorbance was read in the spectrophotometer (490 nm) and the 50% cytotoxic concentration (CC_{50}) was defined as the concentration that reduced cell viability by 50% when compared to untreated controls. CC_{50} values were calculated by a non-linear regression equation using GraphPad Prism software.

The definition of the cytotoxicity used was: $\text{CC}_{50} < 1.0 \mu\text{g/mL}$ —high cytotoxicity; $\text{CC}_{50} 1.0\text{--}10.0 \mu\text{g/mL}$ —moderate cytotoxicity; $\text{CC}_{50} 10.0\text{--}20.0 \mu\text{g/mL}$ —mild cytotoxicity; and $\text{CC}_{50} > 20 \mu\text{g/mL}$ —non-cytotoxic⁸⁵.

Antimicrobial activity. The antimicrobial activity of BPE, 70% ethanol, and the composite (GIC-BPE) were studied against two Gram-positive bacteria, *S. aureus* (ATCC 12692) and *S. mutans* (ATCC 25175), microorganisms causing caries; one Gram-negative bacteria, *A. actinomycetemcomitans* (ATCC 33384), microorganism periodontopathogens; as well as *C. albicans* yeast (ATCC 18804), which causes oral lesions. All microorganisms were donated by the Collection of Reference Microorganisms on Health Surveillance from Oswaldo Cruz Foundation, RJ, Brazil. The susceptibility tests were performed using agar diffusion⁸⁶. A 0.1 mL aliquot of 24 h cultures of *C. albicans* was incubated at 37 °C in Sabouraud dextrose broth (Difco), corresponding to 5.0 turbidity units on the McFarland standard (1.5×10^8 UFC/mL), and seeded in 30 mL Sabouraud dextrose agar (Difco). A 0.1 mL aliquot of overnight cultures of *S. mutans* strains incubated at 37 °C in brain heart infusion (BHI) (Difco), corresponding to 0.5 turbidity units on the McFarland standard, was plated onto 30 mL Mitis salivarius bacitracin agar (Difco). *S. aureus* and *A. actinomycetemcomitans* species were incubated overnight at 37 °C and a 0.1 mL aliquot of each was plated onto 30.0 mL blood agar (Difco) supplemented with hemin/menadione (Sigma). Microorganisms were incubated at 37 °C for 18 h in anaerobic system (Difco).

The antimicrobial activity was measured by the inhibition zones produced. The inoculum was initially standardized to 10^8 CFU/mL (50% transmittance at 580 nm), by transferring colonies from the nutrient agar to sterile saline, and 200 μL of the suspension was homogeneously placed on the surface of 50 mL Mueller–Hinton agar in a 150 mm Petri dish. GIC-BPE samples, measuring 6.0 mm in diameter, were planted on the surface of the agar and incubated at a temperature of 37 °C, in an environment with an atmosphere of 5% CO_2 . Sterile blank disks (CECON) were soaked in 20 μL of the isolated ethanolic BPE (46 $\mu\text{g/mL}$) and applied to the agar surface previously seeded with the microorganisms. Additionally, each plate carried control disks: solvent control (20 μL sterile ethanol), and discs containing 10 $\mu\text{g/mL}$ of chlorhexidine (Sigma) for bacteria and 20 $\mu\text{g/mL}$ of nystatin (Sigma) for yeast that were used as inhibition growth positive controls for comparison with the GIC-BPE sample. After 24 h of incubation at 37 °C, the diameters of the inhibition zones were measured and compared. Tests were performed in triplicate.

Conclusion

In this work we studied the physical–chemical, cytotoxic, antibacterial and mechanical properties of GIC-BPE and we compared the results obtained with those of GIC, frequently used in dental restorative clinics. For the GIC-BPE sample, we also evaluated the flavonoid release profile. The ATR-FTIR results can indicate that the flavonoids present in BPE were incorporated into the ionomer, and the study of the flavonoid release profile showed that the flavonoids were practically all released within 60 h. FTIR and thermal analysis results indicated that an intermolecular interaction exists between the glass-ionomer and BPE. This interaction can explain the slight decrease in mechanical properties of the GIC-BPE sample compared to GIC (176.60 ± 6.46 MPa for GIC vs. 161.17 ± 5.01 MPa for GIC-BPE) and the smaller thermal stability of the GIC-BPE samples when compared with the free extract samples (BPE). The results of cytotoxicity and antimicrobial tests showed that the GIC-BPE has antimicrobial activity at non-cytotoxic concentrations to human fibroblasts cells. The results suggest that the prepared composite may represent a new therapeutic option as an alternative agent available for endodontic treatment. This product has a low cost and is an interesting alternative for use in dental treatment, especially in developing countries where the majority of people use the public health support system.

Received: 26 February 2020; Accepted: 3 December 2020

Published online: 18 December 2020

References

- Ganguly, A. *et al.* Application of diverse natural polymers in the design of oral gels for the treatment of periodontal diseases. *J. Mater. Sci. Mater. Med.* **28**, 39 (2017).
- Listgarten, M. A., Lindhe, J. & Hellden, L. The effect of tetracycline and/or scaling on human periodontal disease: Clinical, microbiological observation. *J. Clin. Periodontol.* **5**, 246–271 (1978).
- Carmona, F. & Pereira, A. M. S. Herbal medicines: Old and new concepts, truths and misunderstandings. *Rev. Bras. Farmacogn.* **23**, 379–385 (2013).
- Wink, M. & Van Wyk, B. E. *Mind-altering and poisonous plants of the world* (Briza Publications, Pretoria, 2008).
- Jain, M. K. *et al.* Specific competitive inhibitor of secreted phospholipase A2 from berries of *Schinus terebinthifolius*. *Phytochemistry* **39**, 537–547 (1995).
- Johann, S. *et al.* Antifungal activity of schinol and a new biphenyl compound isolated from *Schinus terebinthifolius* against the pathogenic fungus *Paracoccidioides brasiliensis*. *Ann. Clin. Microbiol. Antimicrob.* **9**, 30 (2010).
- Morais, T. R. *et al.* Antiparasitic activity of natural and semi-synthetic tirucallane triterpenoids from *Schinus terebinthifolius* (Anacardiaceae): Structure/activity relationships. *Mol.* **19**, 5761–5776 (2014).
- Morais, T. R. *et al.* Application of an ionic liquid in the microwave assisted extraction of cytotoxic metabolites from fruits of *Schinus terebinthifolius* Raddi (Anacardiaceae). *J. Braz. Chem. Soc.* **28**, 492–497 (2017).
- Ceruks, M., Romoff, P., Favero, O. A. & Lago, J. H. G. Constituintes fenólicos polares de *Schinus terebinthifolius* Raddi (anacardiaceae). *Quim. Nova* **30**, 597–599 (2007).

10. Santana, J. S., Sartorelli, P. & Lago, J. H. G. Isolamento e avaliação do potencial citotóxico de derivados fenólicos de *Schinus terebinthifolius* Raddi (anacardiaceae). *Quim. Nova* **35**, 2245–2248 (2012).
11. Lima, M. R. F. *et al.* Anti-bacterial activity of some Brazilian medicinal plants. *J. Ethnopharmacol.* **105**, 137–147 (2006).
12. Ibrahim, M.T., Fobbe, R. & Nolte, J. Chemical composition and biological studies of *Egyptian schinus* molle l. and *Schinus terebinthifolius* Raddi oils. *Bull. Fac. Pharm.* **42**, 289–296 (2004).
13. Uliana, M. P. *et al.* Composition and biological activity of Brazilian rose pepper (*Schinus terebinthifolius* Raddi) leaves. *Ind. Crops Prod.* **83**, 235–240 (2016).
14. Andrade, A. L. *et al.* Glass-ionomer-propolis composites for caries inhibition: Flavonoids release, physical-chemical, antibacterial and mechanical properties. *Biomed. Phys. Eng. Express.* **5**, 027006 (2019).
15. Wilson, A. D. & Kent, B. E. The glass-ionomer cement, a new translucent dental filling material. *J. Appl. Chem. Biotechnol.* **21**, 313–313 (1971).
16. Tuzuner, T., Dimkov, A. & Nicholson JW. The effect of antimicrobial additives on the properties of dental glass-ionomer cements: A review. *Acta Biomater. Odontol. Scand.* **5**, 9–21 (2019).
17. Young, A. M. FTIR investigation of polymerisation and polyacid neutralisation kinetics in resin-modified glass-ionomer dental cements. *Biomaterials* **23**, 3289–3295 (2002).
18. Bertoluzza, A., Fagnano, C., Morelli, M. A., Gottardi, V. & Guglielmi, M. Raman and infrared spectra on silica gel evolving toward glass. *J. Non-Cryst. Solids* **48**, 117–128 (1982).
19. Andrade, A. L., Souza, D. M., Vasconcellos, W. A., Ferreira, R. V. & Domingues, R. Z. Tetracycline and/or hydrocortisone incorporation and release by bioactive glasses compounds. *J. Non-Cryst. Solids* **355**, 811–816 (2009).
20. Matos, M. C., Ilharco, L. M. & Almeida, R. M. The evolution of TEOS to silica-gel and glass by vibrational spectroscopy. *J. Non-Cryst. Solids* **147–148**, 232–237 (1992).
21. Lima, Z.M. *et al.* Effect of *Tamarindus indica* L. and *Manihot esculenta* extracts on antibiotic-resistant bacteria. *Pharmacognosy Res.* **9**, 195–199 (2017).
22. Seifzadeh, N. *et al.* Evaluation of polyphenolic compounds in membrane concentrated pistachio hull extract. *Food Chem.* **277**, 398–406 (2019).
23. Liu, Y. *et al.* Purification and characterization of a novel galloyltransferase involved in catechin galloylation in the tea plant (*Camellia sinensis*). *J. Biol. Chem.* **287**, 44406–44417 (2012).
24. Singh, A., Bajpai, V., Kumar, S., Sharma, K. R. & Kumara, B. Profiling of gallic and ellagic acid derivatives in different plant parts of *Terminalia arjuna* by HPLC-ESI-QTOF-MS/MS. *Nat. Prod. Commun.* **11**, 239–244 (2016).
25. Moraes, S.Z.C. *et al.* Antinociceptive and anti-inflammatory effect of *Poincianella pyramidalis* (Tul.) L.P. Queiroz. *J. Ethnopharmacol.* **254**, 112563 (2020).
26. Yue, W. *et al.* Non-targeted metabolomics reveals distinct chemical compositions among different grades of Bai Mudan white tea. *Food Chem.* **277**, 289–297 (2019).
27. Zhou, Y. *et al.* Antioxidant polyphenols from the seed coats of red sword bean (*Canavalia gladiata* (Jacq.) DC.). *Antioxid.* **8**, 200 (2019).
28. Li, X. *et al.* Covalent bridging of corilagin improves antiferroptosis activity: Comparison with 1,3,4-tri-O-galloyl- β -D-glucopyranose. *ACS Med. Chem. Lett.* **6** (2020).
29. Venter, P., Pasch, H. & Villiers, A. Comprehensive analysis of tara tannins by reversed-phase and hydrophilic interaction chromatography coupled to ion mobility and high-resolution mass spectrometry. *Anal. Bioanal. Chem.* **411**, 6329–6341 (2019).
30. Zhang, D. Y. *et al.* An effective homogenate-assisted negative pressure cavitation extraction for the determination of phenolic compounds in pyrola by LC-MS/MS and the evaluation of its antioxidant activity. *Food Funct.* **6**, 3323–3333 (2015).
31. Sanz, M. *et al.* Phenolic compounds in chestnut (*Castanea sativa* Mill.) heartwood. Effect of toasting at cooperage. *J. Agric. Food Chem.* **58**, 9631–9640 (2010).
32. Chen, H. *et al.* Isolation and identification of the anti-oxidant constituents from *Loropetalum chinense* (R. Brown) Oliv. based on UHPLC-Q-TOF-MS/MS. *Mol.* **23**, 1720 (2018).
33. Freitas, M.A. *et al.* Evaluation of the antifungal activity of the *Licania rigida* leaf ethanolic extract against biofilms formed by *Candida* sp. isolates in acrylic resin discs. *Antibiot.* **8**, 250 (2019).
34. Zhu, Y. T. *et al.* Fast identification of lipase inhibitors in oolong tea by using lipase functionalized Fe₃O₄ magnetic nanoparticles coupled with UPLC-MS/MS. *Food Chem.* **173**, 521–526 (2015).
35. Nijat, D., Abdulla, R., Liu, G.Y., Luo, Y.Q. & Aisa HA. Identification and quantification of Meiguihua oral solution using liquid chromatography combined with hybrid quadrupole-orbitrap and triple quadrupole mass spectrometers. *J. Chromatogr. B.* **1139**, 121992 (2020).
36. Li, J. *et al.* HPLC-MS/MS determination of flavonoids in *Gleditsia* Spina for its quality assessment. *J. Sep. Sci.* **41**, 1752–1763 (2018).
37. Wang, S. *et al.* Composition of peony petal fatty acids and flavonoids and their effect on *Caenorhabditis elegans* lifespan. *Plant Physiol. Biochem.* **155**, 1–12 (2020).
38. Du, Q., Jerz, G. & Winterhalter, P. Preparation of three flavonoids from the bark of *Salix alba* by high-speed countercurrent chromatographic separation. *J. Liq. Chromatogr. Relat. Technol.* **27**, 3257–3264 (2004).
39. Araujo, N. M. P. *et al.* LC-MS/MS screening and identification of bioactive compounds in leaves, pulp and seed from *Eugenis calycina* Cambess. *Food Res. Int.* **137**, 109556 (2020).
40. Dorta, E., Gonzalez, M., Lobo, M.G., Sanchez-Moreno, C. & Ancos, B. Screening of phenolic compounds in by-product extracts from mangoes (*Mangifera indica* L.) by HPLC-ESI-QTOF-MS and multivariate analysis for use as a food ingredient. *Food Res. Int.* **57**, 51–60 (2014).
41. Azizah, M. *et al.* UHPLC-ESI-QTOF-MS/MS-based molecular networking guided isolation and dereplication of antibacterial and antifungal constituents of *Ventilago denticulate*. *Antibiot.* **9**, 606 (2020).
42. Wang, B. *et al.* Transport and metabolic profiling studies of amentoflavone in Caco-2 cells by UHPLC-ESI-MS/MS and UHPLC-ESI-Q-TOF-MS/MS. *J. Pharm. Biomed. Anal.* **189**, 113441 (2020).
43. Demenciano, S.C. *et al.* Antiproliferative activity and antioxidant potential of extracts of *Garcinia gardneriana*. *Mol.* **25**, 3201 (2020).
44. Ko, Y.C., Feng, H.T., Lee, R.J. & Lee, M.R. The determination of flavonoids in *Wikstroemia indica* C. A. Mey. by liquid chromatography with photo-diode array detection and negative electrospray ionization tandem mass spectrometry. *Rapid Commun. Mass Spectrom.* **27**, 59–67 (2013).
45. ISO (International Organization for Standardization), 2009. In: ISO 10993-5-Biological Evaluation of Medical Devices. Part 5: Tests for in Vitro Cytotoxicity, third ed. (Switzerland).
46. Bendaoud, H., Romdhane, M., Souchard, J.P., Cazaux, S. & Bouajila, J. Chemical composition and anticancer and antioxidant activities of *Schinus Molle* L. and *Schinus terebinthifolius* Raddi berries essential oils. *J. Food Sci.* **75**, C466–472 (2010).
47. McNeill, I.C. & Sadeghi, S.M.T. Thermal stability and degradation mechanisms of poly(acrylic acid) and its salts: Part 1. poly(acrylic acid). *Polym. Degrad. Stab.* **29**, 233–246 (1990).
48. McNeill, I.C. & Sadeghi, S.M.T. Thermal stability and degradation mechanisms of poly(acrylic acid) and its salts: Part 3. Magnesium and calcium salts. *Polym. Degrad. Stab.* **30**, 267–282 (1990).

49. Nicholson, J. W. & Wilson, A. D. (1987) Thermal behavior of films of partially neutralized poly (acrylic acid 1: Influence of metal ions. *Br. Polym. J.* **19**, 67–72 (1987).
50. Araujo, A. A. S., Mercuri, L. P., Seixas, S. R. S., Storpirtis, S. & Matos, J. R. Determinação dos teores de umidade e cinzas de amostras comerciais de guaraná utilizando métodos convencionais e análise térmica. *Rev. Bras. Cienc. Farm.* **42**, 269–277 (2006).
51. Lapuerta, M., Hernandez, J. J. & Rodriguez, J. Kinetics of devolatilisation of forestry wastes from thermogravimetric analysis. *Biomass Bioenergy* **27**, 385–391 (2004).
52. Beninca, B. *et al.* Thermal, rheological, and structural behaviors of natural and modified cassava starch granules, with sodium hypochlorite solutions. *J. Therm. Anal. Calorim.* **111**, 2217–2222 (2013).
53. Andrade, M. M. P., Oliveira, C. S., Colman, T. A. D., Costa, F. J. O. G. & Schnitzler, E. Effects of heat moisture on organic cassava starch-thermal, rheological and structural study. *J. Therm. Anal. Calorim.* **115**, 1–8 (2013).
54. Subramaniam, P., Girish Babu, K.L., Neeraja, G. & Pillai, S. Does addition of propolis to glass ionomer cement alter its physico-mechanical properties? An in vitro study. *J. Clin. Pediatr. Dent.* **41**, 62–65 (2017).
55. Valanezhad, A., Odatsu, T., Udoh, K., Shiraiishi, T., Sawase, T. & Watanabe, I. Modification of resin modified glass ionomer cement by addition of bioactive glass nanoparticles. *J. Mater. Sci. Mater. Med.* **27**, 3 (2016).
56. Takahashi, Y. *et al.* Antibacterial effects and physical properties of glass-ionomer cements containing chlorhexidine for the ART approach. *Dent. Mater.* **22**, 647–652 (2006).
57. Deepalakshmi, M., Poorni, S., Miglani, R., Rajamani, I. & Ramachandran, S. Evaluation of the antibacterial and physical properties of glass ionomer cements containing chlorhexidine and cetrimide: An in vitro study. *Indian J. Dent. Res.* **21**, 552–556 (2010).
58. Anstice, H. M., Nicholson, J. W. & Bubb, N. L. Studies on the setting of polyelectrolyte cements part 1: Effect of methanol on a zinc polycarboxylate dental cements. *J. Mater. Sci. Mater. Med.* **5**, 176–179 (1994).
59. Nicholson, J. W. & Abiden, F. Studies on the setting of polyelectrolyte cements, Part VI: The effect of halide salts on the mechanical properties and water balance of zinc polycarboxylate and glass-ionomer dental cements. *J. Mater. Sci. Mater. Med.* **9**, 269–272 (1998).
60. Tabaldi, L. A. *et al.* Biomass yield and flavonoid and phenol content of *Schinus terebinthifolius* cultivated in single or double row with poultry litter. *Ciênc. Florest.* **26**, 787–796 (2016).
61. Taamali, A. *et al.* UPLC–QTOF/MS for a rapid characterization of phenolic compounds from leaves of *Myrtus communis* L. *Phytochem. Anal.* **25**, 89–96 (2014).
62. Gehrke, I. T. S. *et al.* Antimicrobial activity of *Schinus lentiscifolius* (Anacardiaceae). *J. Ethnopharmacol.* **148**, 486–491 (2013).
63. Silva, J. H. S. *et al.* Anti-*Escherichia coli* activity of extracts from *Schinus terebinthifolius* fruits and leaves. *Nat. Prod. Res.* **32**, 1365–1368 (2018).
64. Aissani, N., Coroneo, V., Fattouch, S. & Caboni, P. Inhibitory effect of carob (*Ceratonia siliqua*) leaves methanolic extract on *Listeria monocytogenes*. *J. Agric. Food Chem.* **60**, 9954–9958
65. Marino, A. *et al.* Antimicrobial activities, toxicity and phenolic composition of *Asphodeline anatolica* E. Tuzlaci leaf extracts from Turkey. *Nat. Prod. Res.* **30**, 2620–2623 (2016).
66. As, F.A.S. *et al.* Phytochemical analysis and antimicrobial activity of *Myrcia tomentosa* (Aubl.) DC. Leaves. *Mol.* **22**, 1100 (2017).
67. Hwang, J. H., Choi, H., Woo, E. R. & Lee, D. G. Antibacterial effect of amentoflavone and its synergistic effect with antibiotics. *J. Microbiol. Biotechnol.* **23**, 953–958 (2013).
68. Batycky, R. P., Hanes, J., Langer, R. & Edwards, D. A. A theoretical model of erosion and macromolecular drug release from biodegrading microspheres. *J. Pharm. Sci.* **86**, 1464–1477 (1997).
69. Dimkov, A., Nicholson, J.W., Gjorgievska, E. & Stevanovic, M. Studies on the incorporation of benzalkonium chloride and cetylpyridinium chloride antimicrobial agents into glass-ionomer dental cements. *Res. J. Pharm., Biol. Chem. Sci.* **7**, 920–925 (2016).
70. Mulla, Z., Edwards, M. & Nicholson, J.W. Release of sodium fusidate from glass-ionomer dental cement. *J. Mater. Sci.: Mater. Med.* **21**, 1997–2000 (2010).
71. Leung, D. *et al.* Chlorhexidine-releasing methacrylate dental composite materials. *Biomaterials* **26**, 7145–7153 (2005).
72. Jakobek, L. Interactions of polyphenols with carbohydrates, lipids and proteins. *Food Chem.* **175**, 556–567 (2015).
73. Daglia, M. Polyphenols as antimicrobial agents. *Curr. Opin. Biotechnol.* **23**, 174–181 (2012).
74. Mila, I., Scalbert, A. & Expert, D. Iron withholding by plant polyphenols and resistance to pathogens and rots. *Phytochemistry* **42**, 1551–1555 (1996).
75. Petti, S. & Scully, C. Polyphenols, oral health and disease: A review. *J. Dent.* **37**, 413–423 (2009).
76. International Organization for Standardization. *ISO9917-2:2010 Water-based cements - Part 2: Resin-modified cements* (International Organization for Standardization, Geneva, 2010).
77. Egwaikhide, P. A. & Gimba, C. Analysis of the phytochemical content and anti-microbial activity of *Plectranthus glandulosus* whole plant. *Middle-East J. Sci. Res.* **2**, 135–138 (2007).
78. Bonoli, M., Verardo, V., Marconi, E. & Caboni, M.F. Antioxidant phenols in barley (*Hordeum vulgare* L.) flour: Comparative spectrophotometric study among extraction methods of free and bound phenolic compounds. *J. Agric. Food Chem.* **52**, 5195–5200 (2004).
79. Chang, C. C., Yang, M. H., Wen, H. M. & Chern, J. C. Estimation of total flavonoid content in propolis by two complementary colorimetric methods. *J. Food Drug Anal.* **10**, 178–182 (2002).
80. Andrade, A. L., Manzi, D. & Domingues, R. Z. Tetracycline and propolis incorporation and release by bioactive glassy compounds. *J. Non-Cryst. Solids* **352**, 3502–3507 (2006).
81. Andrade, A.L., Militani, I.A., Almeida, K.J., Belchior, J.C., Reis, S.C., Costa e Silva, R.M.F. & Domingues, R.Z. Theoretical and experimental studies of the controlled release of tetracycline incorporated into bioactive glasses. *AAPS PharmSciTech* **19**, 1287–1296 (2018).
82. Kokubo, T., Kushitani, H., Sakka, S., Kitsugi, T. & Yamamuro, T. Solutions able to reproduce in vivo surface-structure changes in bioactive glass-ceramic A-W3. *J. Biomed. Mater. Res.* **24**, 721–734 (1990).
83. Dowd, L. E. Spectrophotometric determination of quercetin. *Anal. Chem.* **31**, 1184–1187 (1959).
84. Praisin, J. K., Wang, C. C. & Barnes, S. Mass spectrometric methods for the determination of flavonoids in biological samples. *Free Rad. Biol. Med.* **37**, 1324–1350 (2004).
85. Magadula, J. J. & Suleimani, H. O. Cytotoxic and anti-HIV activities of some Tanzanian *Garcinia* species. *Tanzan. J. Health Res.* **12**, 1–7 (2010).
86. Clinical and Laboratory Standards Institute (CLSI). Performance standards for antimicrobial disk susceptibility tests; approved standard, 9th edition. M2-A9. Wayne: Clinical and Laboratory Standards Institute (CLSI); 2006.

Acknowledgements

CNPq; CAPES; FAPEMIG; DEQUI-UFOP; DEGEO-UFOP; PROPP-UFOP.

Author contributions

I.C.P. (student) contributed to the study of the flavonoid release profile. J.B.S. (student) contributed to chromatographic analyses. L.S.P. (student) contributed to chromatographic analyses. V.R.S. (professor) contributed to the

biological studies. R.F.dS. (student) contributed to the in collecting plant sample and identification. L.R.D.S. (student) contributed to the biological studies. T.R.A. (PhD student) contributed to the biological studies. V.M.R.dS. (professor) contributed to the chemistry studies. A.M.dN. (professor) contributed to the in collecting plant sample and identification. W.A.V. (professor) contributed to the biological studies. P.M.A.V. (professor) contributed to the biological studies. A.L.A. (professor) contributed to the designed the study, supervised the laboratory work and contributed to critical reading of the manuscript. All the authors have read the final manuscript and approved the submission.

Competing interests

The authors declare no competing interests.

Additional information

Supplementary Information The online version contains supplementary material available at <https://doi.org/10.1038/s41598-020-79257-3>.

Correspondence and requests for materials should be addressed to Â.L.A.

Reprints and permissions information is available at www.nature.com/reprints.

Publisher's note Springer Nature remains neutral with regard to jurisdictional claims in published maps and institutional affiliations.



Open Access This article is licensed under a Creative Commons Attribution 4.0 International License, which permits use, sharing, adaptation, distribution and reproduction in any medium or format, as long as you give appropriate credit to the original author(s) and the source, provide a link to the Creative Commons licence, and indicate if changes were made. The images or other third party material in this article are included in the article's Creative Commons licence, unless indicated otherwise in a credit line to the material. If material is not included in the article's Creative Commons licence and your intended use is not permitted by statutory regulation or exceeds the permitted use, you will need to obtain permission directly from the copyright holder. To view a copy of this licence, visit <http://creativecommons.org/licenses/by/4.0/>.

© The Author(s) 2020